


Article

A Working Fluid Assessment for a Biomass Organic Rankine Cycle under Different Conditions

Jie Ji ^{1,*}, Jiayu Zhang ¹, Xiaoying Jia ¹, Rundong Ji ², Zhenglin Sheng ², Jingxin Qin ¹, Huanyu Zhao ¹, Jiankang Tang ¹, Jiaoyue Su ² and Yaodong Wang ³ 

¹ Huaiyin Institute of Technology, Huaiyin, Huai'an 223002, China

² Jiangsu Huashui Engineering Detection & Consulting Co., Ltd., Huai'an 223001, China

³ Mechanical Engineering, Energy Systems, Department of Engineering, Durham Energy Institute, Durham University, Durham DH1 3LE, UK

* Correspondence: jijie@hyit.edu.cn

Abstract: Many thermal resources are not reasonably used in the chemical industry's production process. To recover the waste heat from organic waste residue-calcium carbonate (CaCO_3), which is added to inhibit hydrogen production, an organic Rankine cycle (ORC) system is applied in this research. An ORC system can reuse the low-temperature waste heat that is not fully utilized. In this study, the mathematical model of the biomass ORC power generation system is constructed. Five organic working fluids, R11, R113, R123, R141b, and R245fa, were selected from the physical characteristics and safety of working fluids. The system application case is the low-temperature heat absorption in a chemical industry's production process. The system is simulated by Aspen Plus V11 software, so as to study and analyze the influence of different working fluids and working conditions on the system performance and to obtain the preferred working fluids under different working conditions. At the same time, the economic evaluation and entropy method of the system are evaluated by using the investment profit rate PRI from different angles. It can be found that R11 and R141b have advantages, but R11 does not have advantages in environmental aspects. Through research, it is found that it is difficult to have a working fluid that can adapt to the biomass ORC power generation system under any working conditions. This paper can provide a basis for the subsequent research and selection of working fluids in the biomass ORC system.

Keywords: biomass ORC system; working fluid investigation



Citation: Ji, J.; Zhang, J.; Jia, X.; Ji, R.; Sheng, Z.; Qin, J.; Zhao, H.; Tang, J.; Su, J.; Wang, Y. A Working Fluid Assessment for a Biomass Organic Rankine Cycle under Different Conditions. *Energies* **2022**, *15*, 7076. <https://doi.org/10.3390/en15197076>

Academic Editor: Andrea De Pascale

Received: 11 August 2022

Accepted: 22 September 2022

Published: 26 September 2022

Publisher's Note: MDPI stays neutral with regard to jurisdictional claims in published maps and institutional affiliations.



Copyright: © 2022 by the authors. Licensee MDPI, Basel, Switzerland. This article is an open access article distributed under the terms and conditions of the Creative Commons Attribution (CC BY) license (<https://creativecommons.org/licenses/by/4.0/>).

1. Introduction

In the face of a global energy shortage and the sharp deterioration of the living environment, it is urgent to develop renewable energy to replace traditional fossil energy, and the rapid development and rational use of new energy is an inevitable trend [1]. At the same time, the efficient use of existing resources can solve a series of energy problems to some extent. Among them, biomass energy is the fourth energy in the world after coal, oil, and natural gas [2], which can be converted into fuel in three states, solid, gas, and liquid [3]. Moreover, biomass energy also includes the advantages of material circulation, high calorific value, and reducing environmental damage [4], which is more easily realized in practical engineering applications. Industrial production plays a dominant role in energy consumption. According to research statistics, in the production process of the chemical industry, energy consumption accounts for about 70% of the total national energy consumption, and a large number of thermal waste heat resources will be generated. Still, the recovery rate of these industrial thermal waste heat resources is only about 20% [5]. At present, the recovery technology for high-temperature heat resources has been well developed, and it has been applied to different fields [6]. Still, it is difficult to recycle the medium-low temperature heat resource [7]. ORC has the advantages of a low boiling point

of the working fluid and a simple system structure, which can perfectly match the industrial heating resources at medium and low temperatures [8]. ORC is regarded as one of the most inflexible and flexible solutions to utilize thermal resources for power generation [9].

In recent years, many scholars have studied the ORC system. Yan Jianguo et al. [10] selected supercritical organic working fluid R134a as the research object in the ORC system. The flow instability of supercritical organic working fluid R134a under heating conditions was studied. The influence of supercritical organic working fluid R134a on the flow instability was obtained when the pressure, fluid inlet temperature, and heat flux parameters changed. It was found that using supercritical fluid in the ORC system can effectively achieve the purpose of low-temperature heat utilization. Under the background of an ORC system with cyclopentane and R245fa as organic working fluids, Wang Peilun et al. [11] studied the effects of evaporation pressure, undercooling, superheat, inlet and outlet temperature difference of the regenerator liquid working fluids, expander efficiency, and the expansion ratio of the ORC system. Zhou Yaodong et al. [12] proposed a new ORC system, which uses non-azeotropic mixtures R227ea and R245ea. The results show that the new system can absorb more heat from the heat source compared to the traditional ORC system and that the net output power is larger. Linda et al. [13] established a thermal equilibrium and economic models for the solar ORC system to study the system's economy under different working conditions. Mert et al. [14] used stepwise multiple linear regression model (SMLR) and deep learning model (DL) to evaluate the power generation of ORC system in 10 kW ORC system. At the same time, the SMLR, DL, and SMLR-DL models were compared. The results show that the SMLR-DL interoperability method is successful and that the power of the ORC system is estimated with high accuracy. In the research of a biomass-energy-coupled ORC system, Ying Zhengen et al. [15] studied the influence of a biomass boiler on the performance of an ORC system and found that the appropriate regulation of heat transfer oil flow and both inlet and outlet temperature can effectively improve the net output power and thermal efficiency of the ORC system. Zhu Yilin et al. [16] used economic evaluation index to optimize the evaporation temperature of the system's key parameters under the biomass direct combustion ORC cogeneration system, which improved the energy utilization rate and economic benefits of the system.

Compared with foreign countries, China has a late start in the research of the ORC system, which is not only limited by time but also needs to overcome the key technologies. Although there have been a large number of studies on the ORC system in China, there are few studies on recycling waste heat resources in the chemical industry and the ORC system coupled with biomass energy. Most of the studies on ORC systems still remain at the level of solving the thermodynamic properties of the system, and the survey of the performance of ORC systems combined with biomass energy is still relatively backward. Based on this, this paper analyzes the ORC power generation system and the biomass ORC power generation system. By constructing the mathematical system model and using Aspen Plus V11 software to simulate the system, the influence of different working fluids and working conditions on the system performance is analyzed. At the same time, the economic index and comprehensive evaluation index are used to study the system more comprehensively.

2. ORC Power Generation System

2.1. Structure of the ORC Power Generation System

The ORC system uses a low boiling-point organic working fluid to replace the refrigerant vapor-driven expander for work [17], which is suitable for medium-low temperature heating resources [18], such as biomass and solar energy. The system mainly comprises an evaporator, expander, working fluid pump, and condenser [19]. The ORC power system structure is shown in Figure 1. The organic working fluid in the evaporator absorbs the heat generated by medium- and low-temperature resources, converts it into high temperature and high-pressure refrigerant vapor, and then enters the expander for work to drive the generator to generate electricity. The vapor discharged from the expander is condensed by

the condenser, and the liquid working fluid is discharged into the working fluid pump to pressure. The pressurized organic working fluid is returned to the evaporator again so as to realize a thermodynamic cycle.

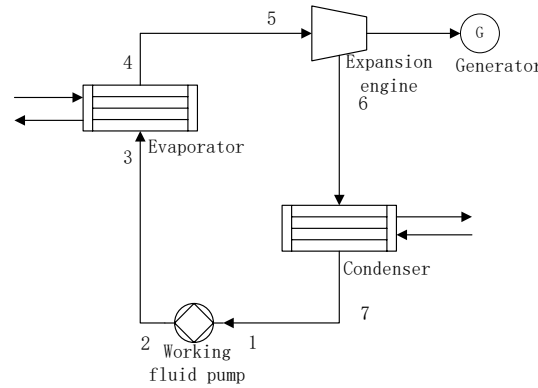


Figure 1. Structure of the ORC power generation system.

2.2. Temperature Entropy Diagram of the ORC Power Generation System

The temperature entropy diagram of the ORC power generation system is shown in Figure 2. Each point marked in the temperature entropy diagram corresponds to a point in the structure diagram of the biomass ORC power generation system. Furthermore, 1–2 is the isentropic compression process in the working fluid pump, but the actual compression process is 1–2. In addition, 2–3–4–5 is the process of the isobaric heat absorption of the working fluid in the evaporator; 5–6 is the isentropic expansion process in the expander, but the actual expansion process is 5–6. The process of the constant pressure condensation of the 6–7–1 working fluid in the condenser.

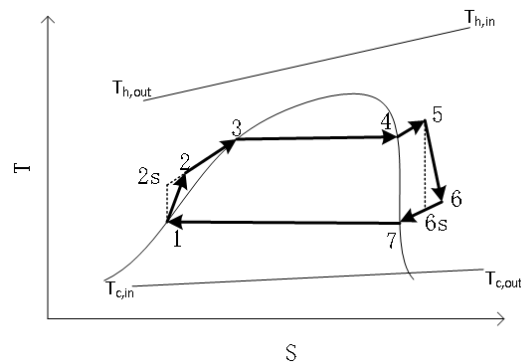


Figure 2. Temperature entropy diagram of the ORC power generation system.

2.3. Mathematical Model of the ORC Power Generation System

The heat absorption of the working fluid in an evaporator is:

$$Q_{eva} = m_f(h_{eva,out} - h_{wmp,out}) = m_g c(T_{in} - T_{out}) \tag{1}$$

In the formula, m_f is the mass flow rate of the working fluid, kg/s; h_z is the enthalpy of each state point z , kJ/kg; m_g is the mass flow of the heat source, kg/s; c is the specific heat capacity of the heat source, kJ/(kg · K); T_{in} , T_{out} is the inlet and outlet temperature of the heat source, K.

The heat release of the working fluid in the condenser is:

$$Q_{con} = m_f(h_{exp,out} - h_{wmp,in}) \tag{2}$$

The expander works as follows:

$$W_{\text{exp}} = m_f \eta_{\text{exp}} (h_{\text{eva},\text{out}} - h_{\text{exp},\text{out}}) \quad (3)$$

In the formula, η_{exp} is the mechanical efficiency of the expander, and the value is 85%. The working fluid pump power is:

$$W_{\text{wmp}} = m_f \eta_{\text{wmp}} (h_{\text{wmp},\text{out}} - h_{\text{wmp},\text{in}}) \quad (4)$$

In the formula, η_{wmp} is the mechanical efficiency of the working fluid pump, and the value is 85%.

3. Biomass ORC Power Generation System

3.1. Biomass ORC Power Generation System Structure

The biomass ORC power generation system is realized by a biomass energy coupled ORC power generation system, and the structure is shown in Figure 3. In this paper, the organic waste residue in the industrial waste heat of the chemical industry is used as the biomass energy, and the biomass fuel enters the biomass boiler for combustion, and calcium carbonate is added to inhibit the generation of hydrogen chloride. The organic working medium in the evaporator uses the heat generated by the biomass boiler to absorb heat and converts it into high-temperature and high-pressure refrigerant vapor. Then it enters the expander to work and drives the generator to generate electricity. The low-temperature and low-pressure refrigerant vapor discharged from the expander enters the condenser into a liquid working medium, then enters the working-medium pump and returns to the evaporator.

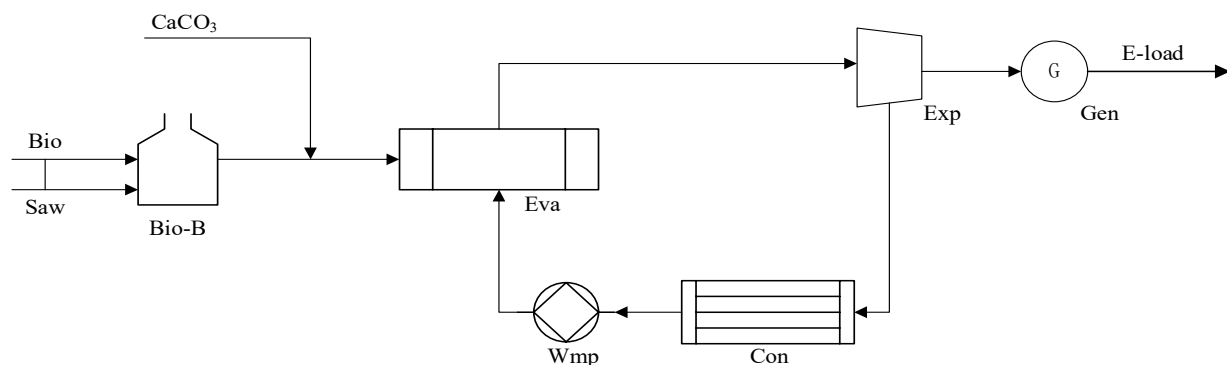


Figure 3. Structure of the biomass ORC power generation system.

3.2. Biomass Boiler Heat Figure

The input and output heat of the biomass boiler is shown in Figure 4. From the perspective of energy change, the biomass boiler can be simply regarded as an energy converter. Through combustion, the chemical energy of chemical organic waste residue is transformed into heat energy. In this paper, heat energy is mainly distributed to organic working fluids and part of it will be discharged into the atmospheric environment.

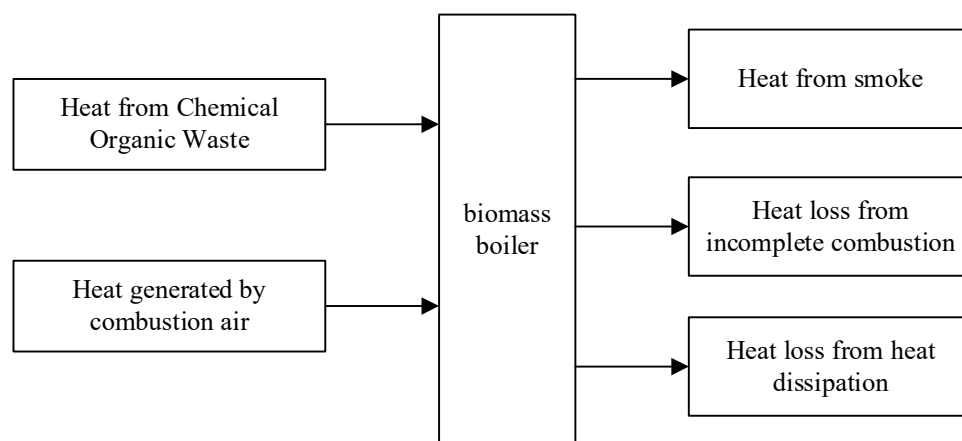


Figure 4. Heat input and output diagram of the biomass boiler.

3.3. Selection of Biomass Energy

In this paper, the residue in the process of the chemical pharmaceutical refrigerant vapor reduction is selected as the fuel of biomass boiler. The residue is basically organic chloride, which will produce secondary pollutants such as hydrogen chloride in combustion [20]. Therefore, calcium carbonate is added to inhibit the generation of hydrogen chloride. The element analysis is shown in Table 1.

Table 1. Element analysis table.

Elementary Analysis	C (%)	H (%)	N (%)	Cl (%)	Low Heating Value (kJ/kg)
Residue	51.2	5.1	6.8	1.1	3680
Chip	46.5	6.5	1.3	-	7026

3.4. Operating Parameters of the Biomass ORC Power Generation System

In this paper, the initial operation parameters of the biomass ORC power generation system are set, and the parameters are shown in Table 2.

Table 2. Initial operation parameters of the system [21].

System Device	Parameter
Biomass fuel	Residue in the refrigerant vapor reduction process
Combustion improver	Chip
Biomass boiler efficiency	90%
Expander efficiency	85%
Working fluid pump efficiency	85%
Ambient pressure	101 KPa
Ambient temperature	20 °C

3.5. Mathematical Model of the Biomass ORC Power Generation System

Under stable working conditions, the input and output heat of the biomass boiler should be conserved, namely

$$Q_{cowr} + Q_{ca} = Q_s + Q_{inc} + Q_{hl} \quad (5)$$

In the formula, Q_{cowr} is the heat generated by chemical organic waste residue, kJ/kg; Q_{ca} is the heat generated by combustion air, kJ/kg; Q_s is the heat taken by the flue gas, kJ/kg; Q_{inc} is the heat loss from incomplete combustion, kJ/kg; Q_{hl} is the heat loss of heat dissipation, kJ/kg.

The heat generated by chemical organic waste is:

$$Q_{cowr} = G_{bio} \times LCV_{bio} \quad (6)$$

In the formula, G_{bio} is the amount of chemical organic waste transported to the biomass boiler, kg/h; LCV_{bio} is the low calorific value of biomass, kJ/kg.

The heat generated by combustion air is:

$$Q_{ca} = 0.8\delta G_{bio}(h_{hs} - h_{ns}) \quad (7)$$

In the formula, δ is the ratio of the actual heating air volume to the theoretical air volume; h_{hs} is the enthalpy in the heating state, kJ/kg; h_{ns} is the enthalpy in the natural state, kJ/kg.

The heat taken away by flue gas is the main heat of the output part of the biomass boiler. The heat generated by flue gas is:

$$Q_s = \eta_{bio-b} V_s c_s \quad (8)$$

In the formula, η_{bio-b} is the efficiency of biomass boiler, and the value is 90%; V_s is the amount of smoke generated, m^3 ; c_s is the specific heat capacity of flue gas, kJ/(kg · K).

The heat loss of incomplete combustion is:

$$Q_{inc} = 2500G_{bio} \times \frac{\eta_{inc}}{100 - \eta_{inc}} \quad (9)$$

In the formula, η_{inc} is the incomplete combustion loss coefficient, %.

The heat loss of heat dissipation is:

$$Q_{hl} = \theta_{bio-b} S_{bio-b} (T_{bc} - T_{env}) \quad (10)$$

In the formula, θ_{bio-b} is the heat transfer coefficient between the wall and the outside of the biomass boiler; S_{bio-b} is the surface area of the biomass boiler wall, m^2 ; T_{bc} is the outer wall temperature of the biomass boiler, K; T_{env} is the environmental temperature, K.

The system heat source mass flow is:

$$m_g = \frac{(Q_{cowr} + Q_{ca}) \times \eta_{bio-b}}{c_w (T_{eva,in} - T_{bio-b,in})} \quad (11)$$

In the formula, c_w is the specific heat capacity of water, kJ/(kg · K).

The mass flow rate of the system working fluid is:

$$m_f = \frac{m_g \times c_w \times (T_{eva,in} - T_{eva,out})}{h_{exp,in} - h_{wmp,out}} \quad (12)$$

3.6. Evaluation Index of System Performance

The net output power of the system is:

$$W_{net} = W_{exp} - W_{wmp} \quad (13)$$

The power generation efficiency of the system is:

$$\eta_{pe} = \frac{W_{net}}{Q_{eva}} \quad (14)$$

The system thermal efficiency is:

$$\eta_{te} = \frac{W_{net}}{Q_{cowr}} \quad (15)$$

The system exergy efficiency is:

$$\eta_e = \frac{W_{net}}{Q_{eva} \left(1 - \frac{T_l}{T_r}\right)} \quad (16)$$

In the formula, $T_r = \frac{T_{in} + T_{out}}{2}$, K; $T_l = \frac{T'_{in} + T'_{out}}{2}$, K.

The irreversible loss is:

$$D = m_f \times T_{env} \times \left(\frac{h_{eva,in} - h_{eva,out}}{T_r} - \frac{h_{wmp,in} - h_{exp,out}}{T_l} \right) \quad (17)$$

4. Selection of Organic Working Fluids for the Biomass ORC Power Generation System

4.1. Classification of Organic Working Fluids

The boiling point of the organic working fluid is generally low, which is suitable for the case of a low-heat source temperature. It is converted into saturated refrigerant vapor by heat absorption, thus driving the expander to work. Organic working fluids are generally divided into three categories: dry working fluids, wet working fluids, and isentropic working fluids [22]. The slope of the saturated refrigerant vapor side curve of the dry working medium in the temperature entropy diagram is positive, such as R123; the slope of the saturated refrigerant vapor side curve of the wet working medium in the temperature entropy diagram is negative, such as carbon dioxide; the slope of the saturated refrigerant vapor side curve of the isentropic working medium in the temperature entropy diagram is 0, such as R245fa. For the biomass ORC system, the dry working medium and the isentropic working medium will be overheating after entering the expander, while the wet working medium will enter the two-phase region, which will cause corrosion to the expander and affect the performance of the expander [23]. Therefore, it is necessary to increase the superheating equipment. Therefore, the dry working medium and the isentropic working medium are generally selected as the circulating working medium of the system. The saturated vapor curves of dry, wet, and isentropic working fluids are shown in Figure 5.

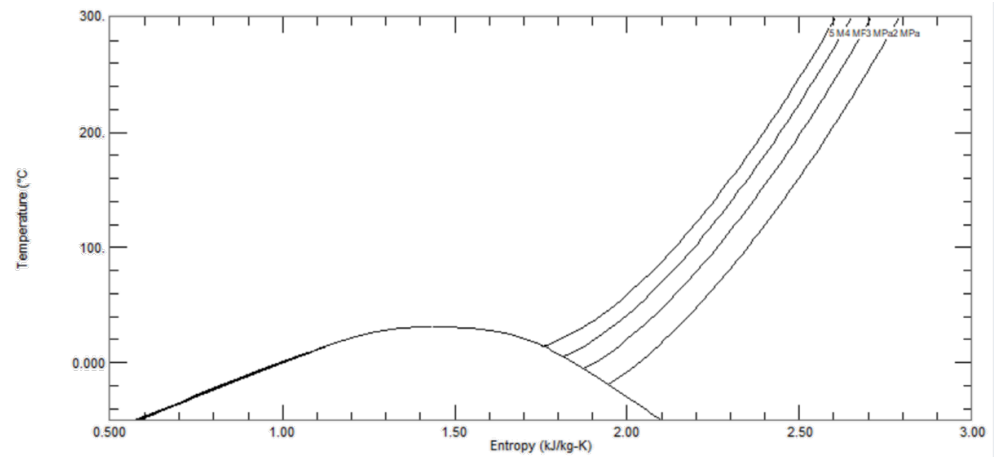
4.2. Selection Principle of Organic Working Fluids

The main factors considered in the principle of selecting organic working fluids include the environmental protection [24] and safety [25] of working fluids, as well as the physical characteristics required for the combination of the biomass ORC system itself, such as small viscosity, large liquid entropy, thermal conductivity, and vaporization latent heat [26]. According to the existing research on organic working fluids, the following common organic working fluids are selected. The physical parameters of organic working fluids are obtained by software REFPROP, as shown in Table 3.

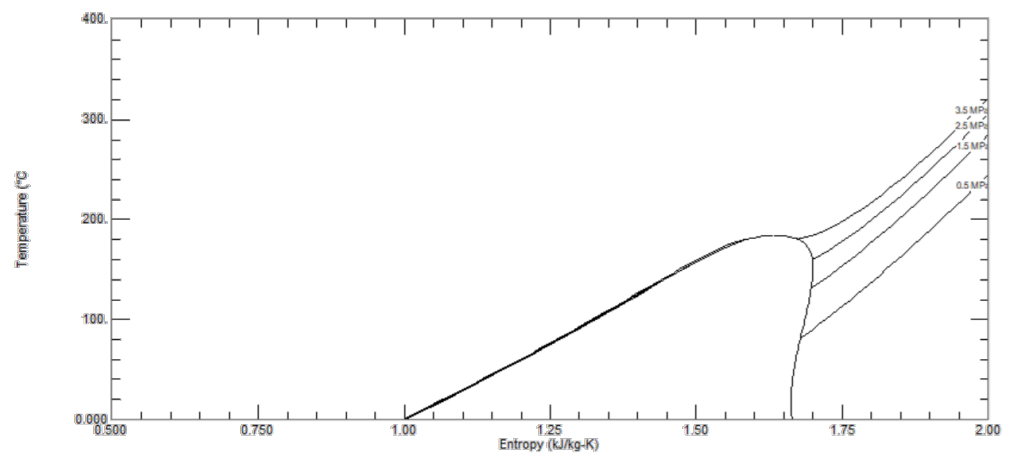
Table 3. Physical parameters table of organic working fluids [27].

Working Substance	Molecular Weight (kg/kmol)	T _{bp} (°C)	T _{ct} (°C)	P _{cp} (Mpa)	Security Property	ODP	GWP
R11	137.37	23.71	197.96	4.41	A1	1.00	4600
R113	187.38	47.59	214.06	3.39	A1	1.00	6130
R123	152.93	27.82	183.68	3.66	B1	0.02	77
R141b	116.95	32.05	204.35	4.21	-	0.09	700
R245fa	134.05	14.9	154.05	3.64	B1	0	1030
R600a	58.12	-11.67	134.67	3.64	A3	0	20
R601a	72.15	27.8	187.2	3.38	A3	0	20
R227ea	170.03	-16.4	102.8	3.00	A1	0	3220

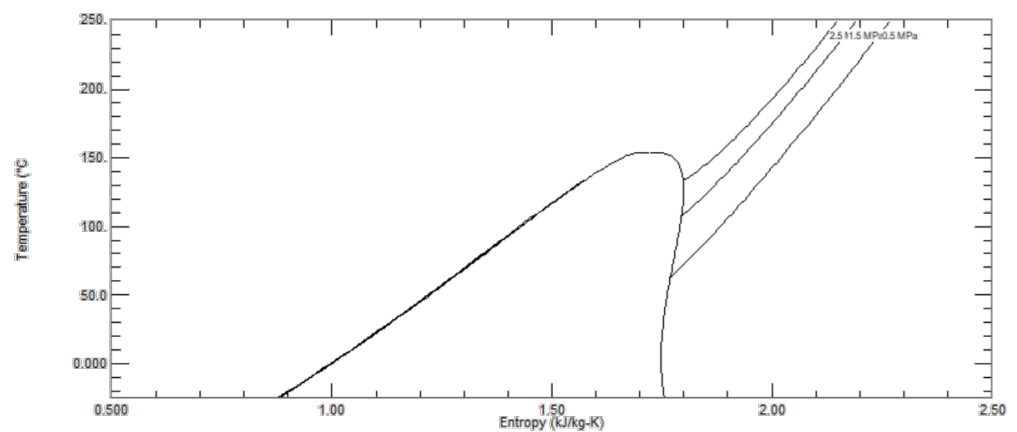
In practical applications, it is difficult to find organic working fluids that meet all the requirements. Therefore, according to the ideal screening principle [28] of organic working fluids, five organic working fluids R123, R11, R113, R245fa, and R141b are proposed.



(a) The saturated vapor curve of R123



(b) The saturated vapor curve of carbon dioxide



(c) The saturated vapor curve of R245fa

Figure 5. Saturated vapor curves of dry, wet, and isentropic working fluids.

4.3. Physical Properties of Organic Working Fluids

Figure 6 shows the physical properties of organic working medium. Figure 6a shows that the viscosity of different organic working fluids varies with evaporation temperature. For the biomass ORC system, the greater the viscosity, the greater the heat-transfer loss caused by the system. Among the five selected working fluids, when the temperature range was 100–150 °C, the viscosity decreased with the increase in temperature. The viscosity of R245fa was the lowest and that of R113 was the highest. The viscosity differences of R11, R123, and R141b were very small.

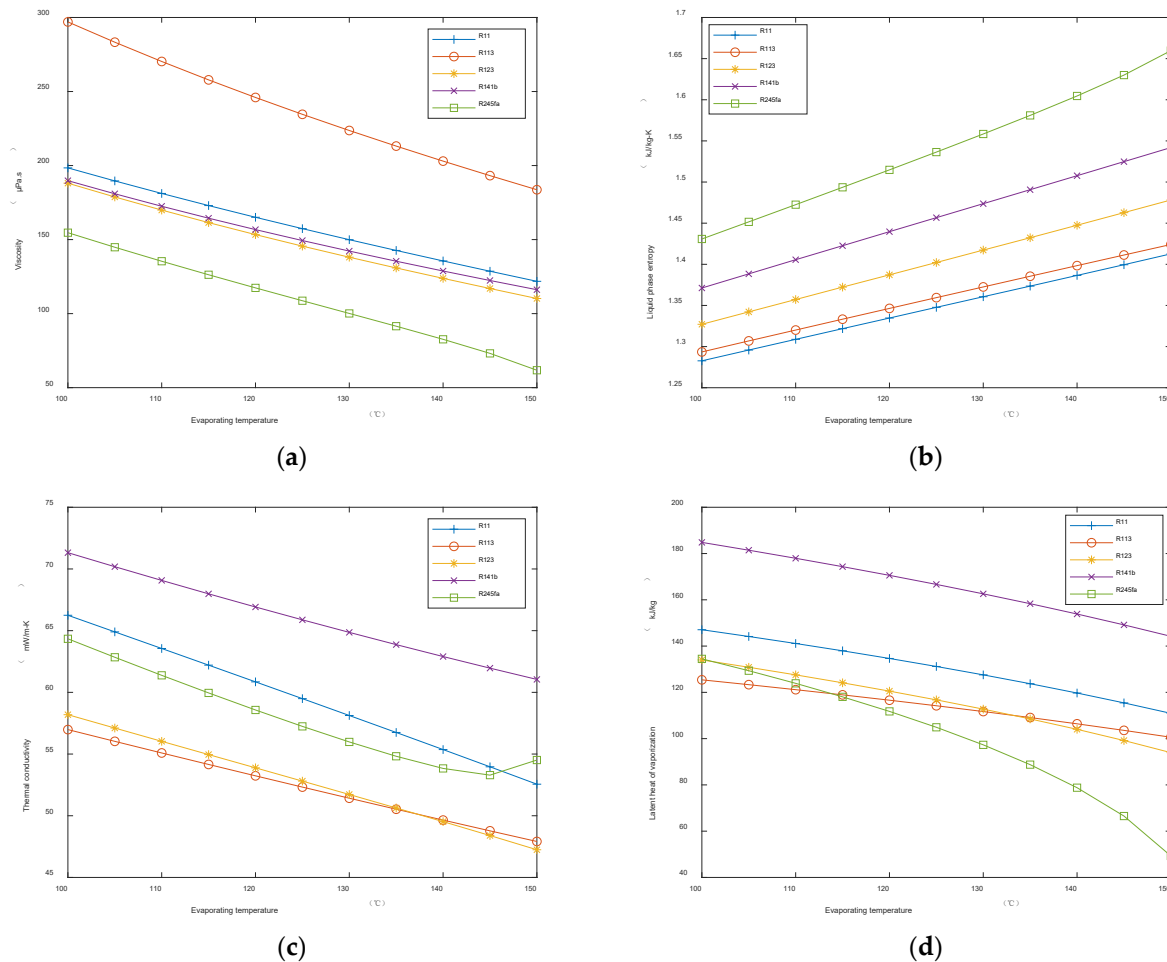


Figure 6. Physical properties of the organic working medium. (a) Variation of viscosity of different organic working fluids with evaporation temperature; (b) Variation of liquid entropy of different organic working fluids with evaporation temperature; (c) The variation of thermal conductivity of different organic working fluids with evaporation temperature; (d) Variation of latent heat of vaporization of different organic working fluids with evaporation temperature.

Figure 6b shows the change in the liquid phase entropy of different organic working fluids with evaporation temperature. In the biomass ORC system, in order to reduce the power consumption of the working fluid pump in the system, the organic working fluid needs large liquid phase entropy. Among the five selected working fluids, when the temperature range was 100–150 °C, the liquid phase entropy increased with the increase in evaporation temperature. Among them, the liquid phase entropy of R245fa was the highest and that of R11 was the lowest.

Figure 6c shows the change in the thermal conductivity of different organic working fluids with evaporation temperature. In the biomass ORC system, the larger the thermal conductivity of organic working fluids is, the better the heat transfer performance is. More-

over, the required heat exchange area of the system is inversely proportional to the thermal conductivity. Therefore, the larger the thermal conductivity is, the better the economic performance of the system is, and the cost is reduced. Among the five selected working fluids, when the temperature range is 100–150 °C, the thermal conductivity decreases with the increase in evaporation temperature. Among them, the thermal conductivity of R141b is the highest and the thermal conductivity of R113 and R123 is the lowest. At the same time, the working fluid R245fa shows a turning point at the evaporation temperature of 145 °C, and increases with the increase in temperature.

Figure 6d shows the change in the vaporization latent heat of different organic working fluids with evaporation temperature. In the biomass ORC system, the vaporization latent heat is the heat absorbed during vaporization. In the selected five working fluids, when the temperature range is 100–150 °C, the vaporization latent heat of organic working fluids decreases with the increase in temperature. Among them, the vaporization latent heat of R141b is the highest; the vaporization latent heat of R113 is the lowest before the evaporation temperature is 115 °C, and the performance of R245fa is the lowest after 115 °C.

5. Effects of Different Organic Working Fluids on the Performance of the Biomass ORC Power Generation System

When choosing suitable organic working fluids, not only the common characteristics of the above conditions should be met, but the target requirements of the system should also be considered, such as net output power, thermal efficiency, exergy efficiency, irreversible loss, investment profit rate, and so on. The most suitable organic working fluid should be selected for different system requirements.

5.1. Effect of the Pressure and Temperature of Different Organic Working Fluids

Figure 7 shows the relationship between pressure and temperature of different organic working fluids. Figure 7a is the relationship between the evaporation pressure of different organic working fluids and the evaporation temperature. The evaporation pressure will affect the mechanical damage and pump power consumption of the system to a certain extent. Therefore, from the perspective of safety and sustainability, organic working fluids with lower evaporation pressure can be selected. It can be seen from the figure that, when the evaporation temperature is set to 80–150 °C, the evaporation pressure of five organic working fluids increases with the increase in evaporation temperature, and the evaporation pressure from high to low is R245fa, R11, R123, R141b, and R113.

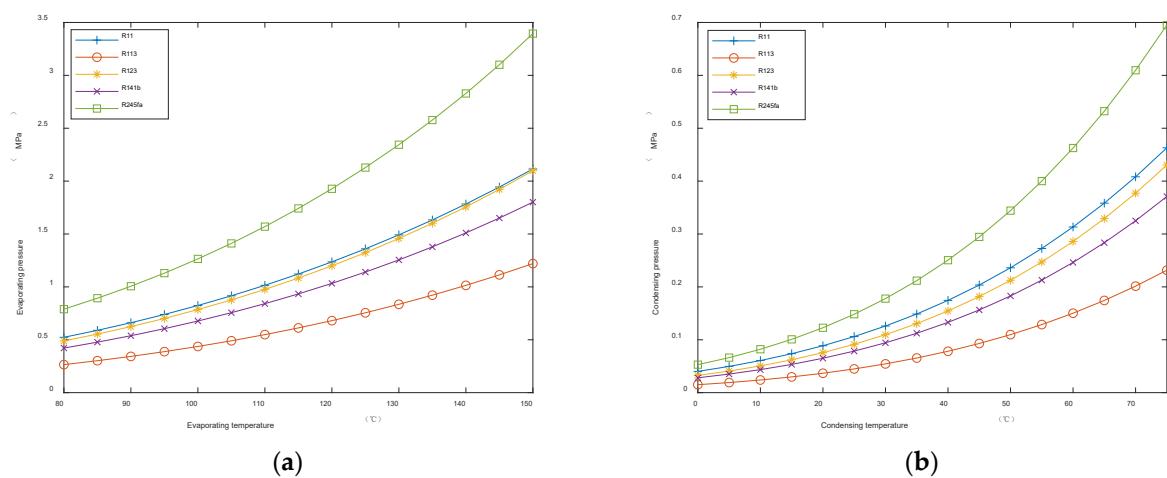


Figure 7. Relationship between the pressure and temperature of different organic working media. (a) Variation of evaporation pressure and evaporation temperature of different organic working fluids. (b) Variation of condensation pressure and temperature for different Organic Working Fluids.

Figure 7b is the relationship between the condensation pressure of different organic refrigerants and the condensation temperature. In the figure, when the condensation temperature range is 0–75 °C, the condensation pressure of the selected five organic refrigerants is proportional to the change of the condensation temperature, and the change trend of the working fluid R245 is more obvious than the other four working fluids. At the same condensation temperature, the condensation pressure of organic refrigerant R245fa is the largest and that of R113 is the smallest. When the condensation temperature is 75 °C, the condensation pressure of R245fa reaches the highest value of 0.695 MPa.

5.2. Effect of the Evaporation Pressure of Different Organic Working Fluids on System Performance

Figure 8 shows the influence of the evaporation pressure of different organic working fluids on system performance. Figure 8a is the change in the thermal efficiency of different organic working fluids with evaporation pressure. When the superheat is 0 °C, the undercooling is 0 °C, the expansion ratio is 4, and the evaporation pressure range is 5–25 bar, the thermal efficiency of five different organic working fluids first increases and then decreases with the increase in evaporation pressure. Among them, within the range of pressure change, R11 has the highest thermal efficiency. Before 21 bar, the lowest thermal efficiency is R245fa; after 21 bar, the lowest is R113. When the pressure is 5 bar, the thermal efficiency of R11 is 9.49%, while that of R245fa is 8.46%. At the same time, the most obvious change trend is the organic working fluid R113. When the pressure increases to 25 bar, the thermal efficiency decreases by 2.37%. Thus, with the thermal efficiency of the system as the first demand, you can consider the choice of organic refrigerant to be R11, R141b, or R123.

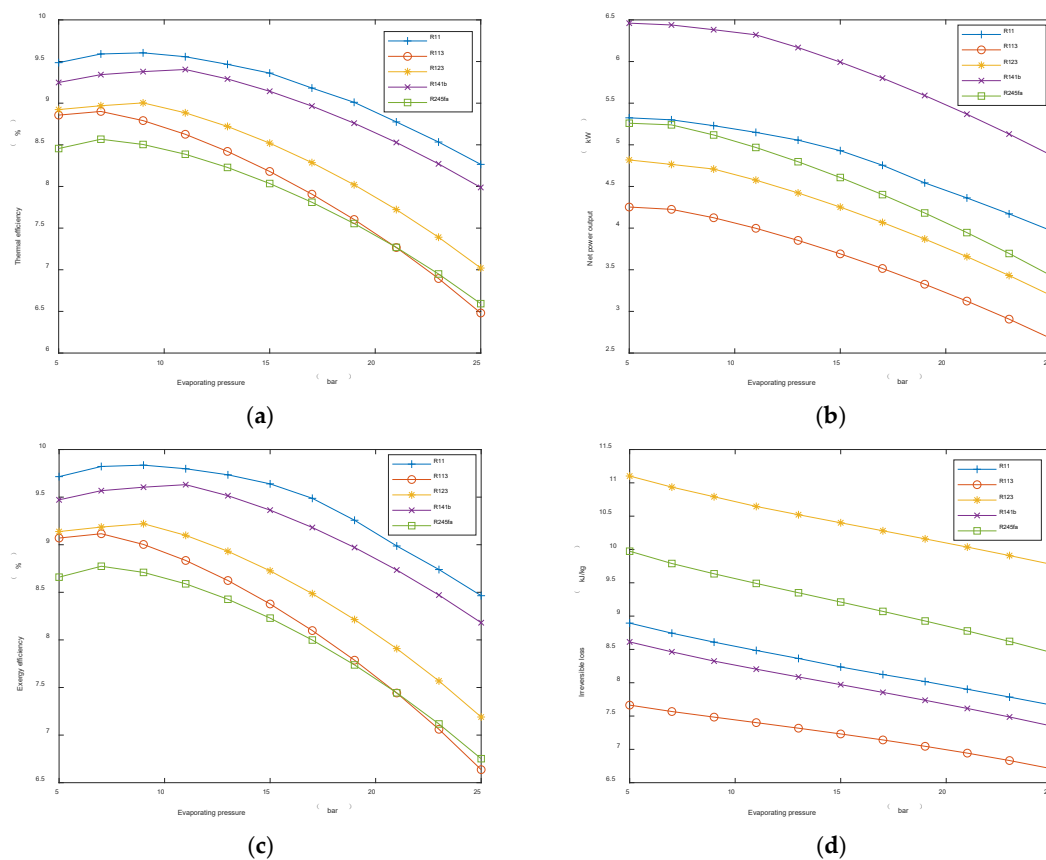


Figure 8. The influence diagram of the evaporation pressure of different organic working fluids on system performance. (a) Effect of evaporation pressure of different organic working fluids on thermal efficiency; (b) Effect of evaporation pressure of different organic working fluids on net output power; (c) Effect of evaporation pressure of different organic working fluids on exergy efficiency (d) Effect of evaporation pressure of different organic working fluids on irreversible loss.

Figure 8b shows the relationship between the net output power of different organic working fluid systems and the evaporation pressure. In the evaporation pressure range of 5–25 bar, the net output power of five different organic working fluids decreases with the increase in evaporation pressure, and the change rate is close. At 5 bar, the lowest net output power is R113; the net output power is 4.25 kW, and the highest is R141b; the net output power is 6.46 kW. When the evaporation pressure increases to 25 bar, the net output power of the five organic working fluids decreases to the lowest point. Among them, the net output power of working fluid R113 is reduced to 2.67 kW and the working fluid R141b is reduced to 4.88 kW. Therefore, when the net output power of the system is the target demand, R141b is preferred, followed by R11.

Figure 8c shows the relationship between the exergy efficiency of different organic working fluid systems and evaporation pressure. When the evaporation pressure range is 5–25 bar, the exergy efficiency of the five working fluids increases first and then decreases with the increase in evaporation pressure. The organic working fluid with the highest exergy efficiency is R11. When the evaporation pressure is 5 bar, the exergy efficiency of the system is 9.72%. When the evaporation pressure is about 9 bar, the exergy efficiency reaches the maximum value of 9.84%. At the same time, R113 has the fastest decline rate. When the evaporation pressure increases to 23 bar, it becomes the organic working fluid with the lowest exergy efficiency of the system, which is about 6.64%. Thus, when the system efficiency is optimal, the most suitable organic working fluids are R11 and R141b.

Figure 8d shows the relationship between the irreversible losses of different organic working fluids and the evaporation pressure. When the evaporation pressure varies from 5 bar to 25 bar, the irreversible loss of the five working fluids decreases with the increase in evaporation pressure. The irreversible loss of working fluid R123 is the highest in the range of variation, which is about 11.1 kJ/kg at 5 bar. When the evaporation pressure increases to 25 bar, the irreversible loss decreased to about 9.78 kJ/kg, which decreased by 1.32 kJ/kg. The lowest irreversible loss is R113; when the pressure is 5–25 bar, the irreversible loss value is reduced from 7.66 to 6.71 kJ/kg. Therefore, when the irreversible loss of the system is taken as the objective, the optimal working fluid is R113, followed by R141b and R11.

5.3. Effect of the Expansion Ratios of Different Organic Working Fluids on System Performance

Figure 9 shows the effect of different organic working fluid expansion ratios on system performance. Figure 9a shows the curves of the system thermal efficiency of different organic working fluids with the expansion ratio. When the evaporation pressure is 5 bar, the superheat is 10 °C, the supercooling is 0 °C, and the expansion ratio is 1.3–4, the system thermal efficiency of the five organic working fluids increases with the increase of the expansion ratio, and the values are very close. When the expansion ratio increases from 1.3 to 4, the system thermal efficiency of working fluid R11 is higher than that of its four organic working fluids, from 2.34 to 9.55%, increasing by 7.21%. Among them, the thermal efficiency values of working fluid R123 and R113 are basically the same, and the lowest is R245fa. When the expansion ratio is 1.3, the thermal efficiency is 2.08%. When the expansion ratio increases to 4, the value also increases to 8.45%. Thus, when the thermal efficiency of the system is the highest, the working fluid R11 is preferred.

Figure 9b is the relationship between the net output power of different organic working fluids and the expansion ratio. When the other conditions of the system are unchanged and the expansion ratio changes in the 1.3–4 range, the net output power of the five organic working fluids increases with the increase in the expansion ratio. The net output power of R141b is the highest. When the expansion ratio is 1.3, the net output power is 1.38 kW. When the expansion ratio is 4, the net output power increases to 6.73 kW. Next are working fluids R11 and R245fa, and the net output power is very close in the range of the expansion ratio set by the system. The lowest net output power is R113, and the growth rate is the smallest. In the range of expansion ratio 1.3–4, the value increases from 0.87 to 4.42 kW, which increases by 3.55 kW. Therefore, when the net output power of the system is selected as the priority target, the working fluids R141b, R11, and R245fa are preferred.

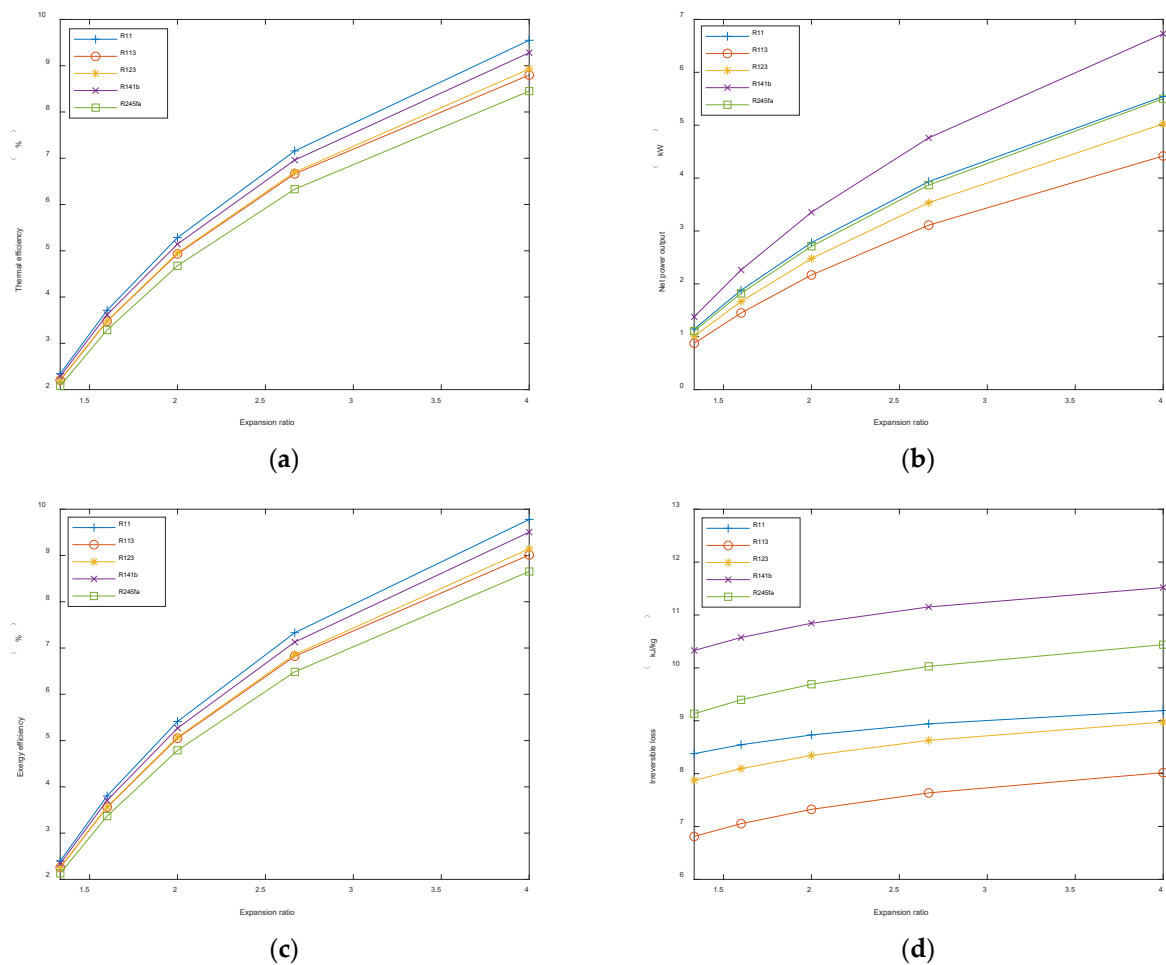


Figure 9. The influence diagram of different organic refrigerant expansion ratios on system performance. (a) The effect of expansion ratio of different organic working fluids on thermal efficiency; (b) The effect of different organic expansion ratio on the net output power; (c) Effect of expansion ratio of different organic working fluids on exergy efficiency; (d) The effect of different organic expansion ratios on irreversible loss.

Figure 9c is the curve of efficiency versus the expansion ratio for different organic working fluids. When the expansion ratio is set in the range of 1.3–4, the efficiency of five working fluids is very close and increases with the increase in the expansion ratio. Among them, the maximum efficiency of working fluid R11, its efficiency value increasing from 2.4 to 9.78%, increased by 7.38%. The second is working fluid R141b. When the expansion ratio changes between 1.3 and 4, the exergy efficiency increases from 2.34 to 9.5%. The exergy efficiency of working fluid R113 and R123 is basically the same. When the expansion ratio increases to three, the exergy efficiency of R123 is slightly higher than that of R113. Therefore, when the system efficiency is selected as the objective function, the working fluids R11 and R141b are better than the other three working fluids.

Figure 9d shows the change of the irreversible loss of the system with the expansion ratio. When other working conditions of the system remain unchanged and the expansion ratio is set between 1.3 and 4, the irreversible loss of the five organic working fluids increases slowly with the increase in the expansion ratio. The working fluid R113 has the smallest irreversible loss. When the expansion ratio is 1.3, the irreversible loss is 6.81 kJ/kg. When the expansion ratio increases to 4, the irreversible loss also increases to 8.02 kJ/kg. The second was R123. In the range of the expansion ratio, the irreversible loss value increased from 7.87 to 9.97 kJ/kg, increasing by 1.1 kJ/kg. The working fluid R141b has the

highest irreversible loss value, so the working fluid R113 and R123 are preferred when the irreversible loss value is selected as the first target.

5.4. Results and Discussion

Through the research and analysis of a biomass ORC power generation system under different working conditions, it can be found that, when the evaporation pressure and the expansion ratio are parameters, the change trend of the system performance index curve is obvious, which has a great influence on the system. When the system requirements are different, the preferred organic refrigerants are also different. For example, when the thermal efficiency is the priority target, R11 can be selected. When the net output power is the first demand, R141b can be selected. When the exergy efficiency is the first choice, R11 can be selected. When the irreversible loss is given priority, R113 is selected.

5.5. Verification of the Model

Table 4 shows the accuracy verification results of the simulation model. Although the system model in this paper is not completely consistent with the reference article, some basic parameter settings in the model can be set as the parameter values in the reference article to verify the accuracy of the model. It can be seen from Table 4 that when the model parameters in this paper are set according to the control model parameters in the reference, the error of the system operation results is less than 1%. Therefore, the simulation model established in this paper can be applied to the following work.

Table 4. Model validation.

System Setting Parameters	Expander Efficiency (%)	Working Fluid Pump Efficiency (%)	Working Substance	Evaporating Temperature (°C)	Thermal Efficiency (%)	Net Power Output (kW)
This thesis	85	85	R11	150	15.85	8.52
1 ref [23]	85	85	R11	150	17.28	7.69
Error (%)	-	-	-	-	0.08	0.11

6. Economic Evaluation Index of the Biomass ORC Power Generation System

6.1. Economic Evaluation Indicator Model

The total system cost is:

$$C_{sys} = C_{tot} + C_{ope-mai} \quad (18)$$

In the form, C_{tot} is the main equipment cost of the system, and $C_{ope-mai}$ is the system operation and maintenance cost.

$$C_{equ} = C_b F_{equ} \quad (19)$$

In the formula, C_b is the base cost, and F_{equ} is the composite factor.

$$\lg C_b = K_1 + K_2 \lg M + K_3 (\lg M)^2 \quad (20)$$

In the formula, K_1 , K_2 , K_3 is the equipment cost calculation coefficient; M is the characteristic parameter of each equipment, and the evaporator and condenser are the heat exchange area, m^2 ; the expander and working fluid pump are the work size, kW .

$$F_{equ} = B_1 + B_2 F_o F_P \quad (21)$$

In the formula, B_1 , B_2 is the correlation coefficient of each device; F_o is the equipment material factor; F_P is the equipment pressure factor.

$$\lg F_P = A_1 + A_2 \lg P + A_3 (\lg P)^2 \quad (22)$$

In the formula, A_1, A_2, A_3 is the pressure factor calculation coefficient of each equipment; P bears the pressure for each equipment under working conditions, *bar*.

$$C_{equ} = C_{equ,eva} + C_{equ,con} + C_{equ,exp} + C_{equ,wmp} \quad (23)$$

$$C_{tot} = C_{equ}CEPCI_{2019}/CEPCI_{1996} \quad (24)$$

$$C_{ope-mai} = 0.015C_{tot} \quad (25)$$

In the formula, $CEPCI$ is the chemical cost index; $CEPCI_{1996}$ is 382; $CEPCI_{2019}$ is 607. The annual income of the system is:

$$INC = W_{net}He \quad (26)$$

In the formula, H is the annual operation hours of the system, and the value is 8000 h; e is the electricity price with a value of 0.15 \$/kW · h.

The annual net income of the system is:

$$NAI = INC - C_{ope-mai} \quad (27)$$

The system investment profit rate is:

$$PRI = \frac{NAI}{C_{tot}} \quad (28)$$

6.2. Economic Evaluation Indexes of Different Organic Working Fluids

Figure 10 shows the economic evaluation index curves of five different organic working fluids under different evaporation pressures. The superheat, undercooling, and expansion ratio of the biomass ORC power generation system are set as fixed values, and the evaporation pressure changes between 5 bar and 25 bar. It can be seen from the figure that, with the increase in evaporation pressure, the investment profit margins PRI of the five working fluids decrease. Among the five working fluids, the working fluid R141b has the highest investment profit rate. When the evaporation pressure is 5 bar, the PRI value is about 26.55%, and when the evaporation pressure increases to 25 bar, the PRI value decreases to 18.91%. The second is working fluid R11, which decreases from 21.98 to 15.35% in the range of evaporation pressure. Thus, considering the system economy as the evaluation index, the working fluids R141b and R11 are preferred.

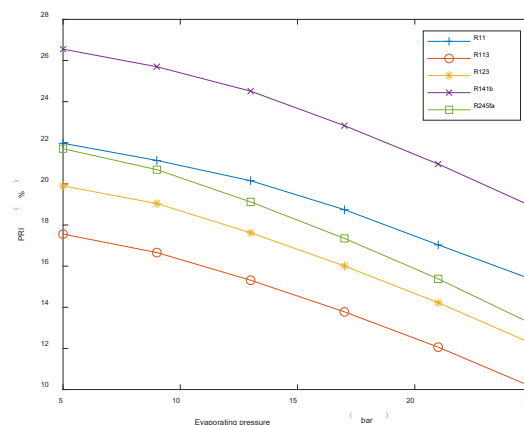


Figure 10. Effect of the evaporation pressure of different organic working fluids on investment profit rate PRI.

7. Comprehensive Evaluation Index of the Biomass ORC Power Generation System

7.1. System Comprehensive Evaluation Index Model

In the previous part, multiple system evaluation indices are involved, such as net output power, thermal efficiency, exergy efficiency, irreversible loss, investment profit margin PRI, and other objective functions. However, the evaluation of the system using a single objective function is not comprehensive, so it is necessary to comprehensively consider these evaluation indices. Therefore, this paper establishes a comprehensive evaluation index model [29]. In view of the original entropy method [30], the improved simplified entropy method is used to evaluate the system more comprehensively, including data standardization, the information entropy value of each index and, the information utility value, and then the weight and comprehensive evaluation index function are obtained. The overall performance of the system should be considered.

For the net output power, the thermal efficiency, exergy efficiency, and investment profit rate of the system, the larger the value of the evaluation index is, the better it is. Therefore, when the four indices are standardized, the membership degree is:

$$x_{ij} = \frac{X_{ij} - \min X_{ij}}{\max X_{ij} - \min X_{ij}} \quad (29)$$

In the formula, X_{ij} is the j th evaluation index value in the i th sample, $0 \leq i \leq a$, $0 \leq j \leq n$; a is the sample size, and n is the number of evaluation indexes.

For irreversible loss, the smaller the evaluation index value is, the better it is. Therefore, when the irreversible loss index is standardized, its membership degree is:

$$x_{ij} = \frac{\max X_{ij} - X_{ij}}{\max X_{ij} - \min X_{ij}} \quad (30)$$

The information entropy value is:

$$p_j = -\frac{1}{\ln(a)} \times \sum_{i=1}^a x_{ij} \ln(x_{ij}) \quad (31)$$

The information utility value is:

$$u_j = 1 - p_j \quad (32)$$

The weight coefficient is:

$$\omega_j = \frac{u_j}{\sum_{j=1}^n u_j} \quad (33)$$

The comprehensive evaluation index function is:

$$L(i) = \sum_{j=1}^n (x_{ij} \times \omega_j) \quad (34)$$

7.2. Comprehensive Evaluation Indices of Different Organic Working Fluids

Figure 11 shows the comprehensive evaluation indices of different organic working fluids under different evaporation pressures. The evaporation pressure of the system varies from 5 bar to 25 bar, and other set values remain unchanged. In the figure, the comprehensive evaluation indexes of R11, R113, and R141b increase with the increase in evaporation pressure, while the working fluids R123 and R245fa show a downward trend after about 21 bar. Among the five working fluids, the comprehensive evaluation index values of R11 and R141b are significantly higher than those of the other three working fluids, and the comprehensive evaluation index values of the two working fluids are very

close in the range of evaporation pressure. The working fluid R11 increases from 1.828 to 1.913, while R141b increases from 1.839 to 1.909. When the evaporation pressure increases to about 20 bar, the comprehensive evaluation index value of R11 exceeds R141b. Therefore, considering the influence of different working fluids on the performance of the system under different working conditions, working fluids R11 and R141b are significantly better than other working fluids.

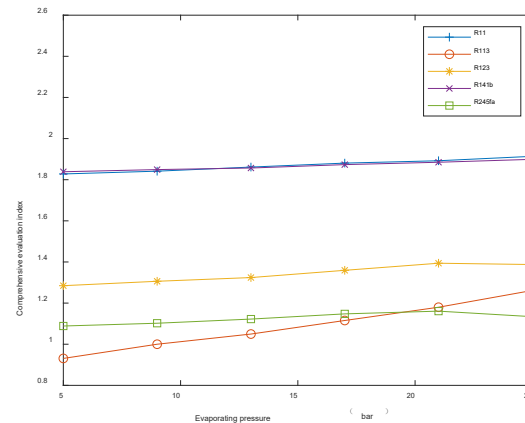


Figure 11. Effect of the evaporation pressure of different organic working fluids on the comprehensive evaluation index.

8. Conclusions

This paper selected the organic waste residue generated in chemical and pharmaceutical refrigerant vapor reduction as the biomass fuel. Because of the particularity of the fuel, calcium carbonate is added to inhibit secondary pollutants such as hydrogen chloride from investigating the performance of the biomass ORC power generation system. Aspen Plus V11 was used to simulate it. Five kinds of organic working fluids (R11, R113, R123, R141b, and R245fa) were introduced. At the same time, the thermal efficiency, net output power, exergy efficiency, irreversible loss, economic evaluation index PRI, and comprehensive evaluation index were selected to analyze the influence of different working fluids on them under different system conditions (evaporation pressure and expansion ratio). It provides a basis for the research and selection of working fluids for the subsequent biomass ORC power generation system.

Through research, the following conclusions are drawn:

(1) Among the five selected organic working fluids, the control variable method is adopted for the biomass ORC power generation system under different working conditions. Namely, the evaporation pressure and irreversible loss are the single variables of the system. Under the two modes, the working fluid R11 has the highest system thermal efficiency and exergy efficiency, which are about 9.55 and 9.84%, respectively. The working fluid R141b has the most significant net output power, about 7.24 kW. The working fluid R113 has a minor irreversible loss, about 6.71 kJ/kg.

(2) The influence of five organic working fluids on the system performance under different working conditions is analyzed. It is found that the evaporation pressure and expansion ratio have a great influence on the system index (thermal efficiency, net output power, exergy efficiency, and irreversible loss), and the changing trend is obvious.

(3) The investment profit margin PRI is used as the economic index of the biomass ORC power generation system to further evaluate the system. It can be seen from the results that the economic index evaluation of R141b is the best and that the PRI value is about 26.55%.

(4) In order to evaluate the biomass organic Rankine cycle power generation system more comprehensively, the improved simplified entropy method is used as the comprehensive evaluation index of the system. It is found that R11 and R141b are better, but R11 is not ideal in the environment.

(5) The study of these five working fluid found that no working fluid in any conditions of the biomass organic Rankine cycle power generation system is optimal; thus, when the system has different needs, the choice of working fluid is different.

Author Contributions: Conceptualization, R.J.; Data curation, H.Z.; Formal analysis, X.J.; Investigation, J.T.; Methodology, J.Q.; Project administration, J.J.; Resources, R.J.; Supervision, Y.W.; Validation, J.Q.; Writing—original draft, J.Z.; Writing—review & editing, Z.S. and J.S. All authors have read and agreed to the published version of the manuscript.

Funding: This research received no external funding.

Data Availability Statement: The simulation data used to support the funding of this study are available from the corresponding author upon request.

Conflicts of Interest: The authors declare no conflict of interest.

Nomenclature

English letters

<i>A</i>	Calculation coefficient of an equipment pressure factor
<i>a</i>	Sample size
<i>B</i>	Equipment correlation coefficient
<i>C</i>	Cost (\$)
<i>CEPCI</i>	Chemical cost index
<i>c</i>	Specific heat capacity (kJ/(kg · K))
<i>D</i>	Irreversible loss (kJ/kg)
<i>e</i>	Electrovalence (\$/kW · h)
<i>F</i>	Equipment factor
<i>G</i>	Chemical organic waste residue (kg/h)
<i>H</i>	System annual operation time (h)
<i>h</i>	Enthalpy value (kJ/kg)
<i>INC</i>	Annual earnings (\$)
<i>K</i>	Equipment cost calculation factor
<i>L</i>	Comprehensive evaluation index function
<i>LCV</i>	Low heating value (kJ/kg)
<i>M</i>	Equipment characteristic parameters
<i>m</i>	Mass flow (kg/s)
<i>n</i>	Number of evaluation indicators
<i>NAI</i>	Annual net profit (\$)
<i>P</i>	Pressure (<i>bar</i>)
<i>p</i>	Information entropy value
<i>PRI</i>	Investment profit ratio (%)
<i>Q</i>	Quantity of heat (kJ/kg)
<i>R</i>	Correlation coefficient
<i>S</i>	Surface area (m ²)
<i>T</i>	Temperature (K)
<i>u</i>	Information utility value
<i>V</i>	Volume (m ³)
<i>W</i>	Work (kW)
<i>X</i>	Evaluation index value
<i>x</i>	Membership
Greek alphabet	
η	Efficiency (%)
∂	Ratio of actual heating air volume to theoretical air volume
θ	Coefficient of heat transfer
ω	Weight coefficient

Superscript/Subscript	
<i>b</i>	Bench mark
ω	Weight coefficient
Superscript/Subscript	
<i>b</i>	Bench mark
<i>bc</i>	The external wall of the biomass boiler
<i>bio</i>	Biomass
<i>bio – b</i>	Biomass boiler
<i>ca</i>	Oxidizing air
<i>con</i>	Condenser
<i>cowr</i>	Organic waste residue
<i>e</i>	Exergy
<i>env</i>	Environment
<i>equ</i>	Equipment
<i>eva</i>	Evaporator
<i>exp</i>	Expansion engine
<i>f</i>	Working substance
<i>g</i>	Heat source
<i>hl</i>	Heat dissipation
<i>hs</i>	Heating condition
<i>i</i>	Sample order
<i>in</i>	Import
<i>inc</i>	Incomplete combustion
<i>j</i>	Order of evaluation indices
<i>l</i>	Lower point
<i>net</i>	Net output
<i>ns</i>	Raw state
<i>o</i>	Material
<i>ope – mai</i>	Operation and maintenance
<i>out</i>	Exit
<i>pe</i>	Power generation
<i>r</i>	Higher point
<i>s</i>	Flue gas
<i>sys</i>	System
<i>te</i>	Heat supply
<i>tot</i>	Total system main equipment
<i>w</i>	Water
<i>wmp</i>	Working fluid pump
<i>z</i>	Each state point

References

1. Wang, Z.L.; Cui, Q.J.; Cui, J.H.; Li, X.C.; Jia, G.C.; Sun, Z.H. Design and teaching application of thermodynamic cycle virtual simulation system based on Aspen Plus. *Exp. Technol. Manag.* **2021**, *38*, 218–222.
2. Li, Z.S.; Li, W.Y.; Zhao, J.W.; Shan, D.L. Parameter optimization and comprehensive analysis of biomass-driven ORC triple supply system. *J. Sol. Energy* **2020**, *41*, 375–381.
3. Ge, Y.F.; Qi, Y.X.; Zhang, F.; Li, Y.Y. Experimental study on PVTx properties of new organic Rankine cycle refrigerant R245fa/R152a. *J. Eng. Thermophys.* **2021**, *42*, 2764–2770.
4. Xu, W.; Tao, J.; Yang, H.D.; Tang, W.Q.; Qin, H.R. Optimization of cold—Heat linkage system with biomass energy. *Sci. Technol. Eng.* **2022**, *22*, 6139–6148.
5. An, M.Y.; Zhao, X.R.; Xu, Z.Y.; Wang, R.Z. Coupled compression-absorption high temperature heat pump cycle with industrial heat recovery. *J. Shanghai Jiao Tong Univ.* **2021**, *55*, 434–443.
6. Jie, J.; Xin, X.; Wei, N.; Ni, W.; Teng, K.; Miao, C.; Wang, Y.; Roskilly, T. An Experimental and Simulation Study on Optimisation of the Operation of a Distributed Power Generation System with Energy Storage—Meeting Dynamic Household Electricity Demand. *Energies* **2019**, *12*, 1091. [[CrossRef](#)]
7. Huang, L.; Zhao, P.P.; Zhou, D.; Wu, J.F.; Sun, Y.; Qiao, Y.J. The application of ORC-vapor compression coupled refrigeration system in small refrigerated vehicles. *Refrig. Air Cond.* **2021**, *21*, 46–49.
8. Liu, H.L.; Wang, Z.Q.; Liu, X.J.; He, J.X.; Lei, J.Y. Based on the analysis of variable working condition characteristics of organic refrigerant scroll expander. *Energy Sav.* **2021**, *40*, 19–22.

9. Sun, Z. The Experimental and Simulation Study of Micro Organic Rankine Cycle System. Master's Thesis, Beijing Jianzhu University, Beijing, China, 2020.
10. Yan, J.G.; Guo, P.C. Experimental study on flow instability of supercritical fluid in horizontal heating channel. In Proceedings of the Thirty-First National Hydrodynamics Symposium (Volume I), Xiamen, China, 30 October 2020; p. 618623. [[CrossRef](#)]
11. Wang, P.L.; Kong, X.H.; Li, M.; Sui, B.; Wen, Z.Y.; Li, Z.J. Effects of different heats on thermal recovery of organic Rankine cycle. *Intern. Combust. Engine Power Plant* **2020**, *37*, 9–15. [[CrossRef](#)]
12. Zhou, Y.D. Thermodynamics of Partially Evaporated Organic Rankine Cycle with Nonazeotropic Mixtures. Ph.D. Thesis, Shanghai Jiaotong University, Shanghai, China, 2019.
13. Lin, D.; Gu, D.Q.; Zhou, Y.H.; Luo, C.X.; Zhang, H.Z.; Wang, M.X. The technical and economic analysis of solar organic Rankine cycle system. *Zhejiang Electr. Power* **2022**, *41*, 14–19. [[CrossRef](#)]
14. İlker, M.; Huseyin, B.H.; Hüseyin, Y.; Koç, Y. Deep neural network approach to estimation of power production for an organic Rankine cycle system. *J. Braz. Soc. Mech. Sci. Eng.* **2020**, *42*, 620.
15. Ying, Z.G.; Yang, X.J.; Tang, Y. Thermal performance analysis of biomass organic Rankine power generation system. *Energy Eng.* **2017**, *2017*, 32–38. [[CrossRef](#)]
16. Zhu, Y.L.; Wang, Y.Z.; Zhang, X.J.; Li, W.Y.; Li, J.; Li, H.J. The thermal economic analysis of biomass organic Rankine cycle cogeneration system. *Sol. Energy J.* **2020**, *42*, 312–319. [[CrossRef](#)]
17. Zhao, J.L.; Qin, H. Overview of organic Rankine cycle low temperature thermal power generation system. *Mod. Commer. Ind.* **2020**, *41*, 199–200. [[CrossRef](#)]
18. Hu, G.H.; Li, Y.; Chen, Y.; Zhang, L.L. Organic Rankine cycle simulation and optimization of low temperature exergy thermal recovery. *Tianjin Chem. Ind.* **2022**, *36*, 118–121.
19. Zhang, X.; Wang, X.; Cai, J.; He, Z.; Tian, H.; Shu, G.; Shi, L. Experimental study on operating parameters matching characteristic of the organic Rankine cycle for engine waste heat recovery. *Energy* **2022**, *244*, 122681. [[CrossRef](#)]
20. Li, J.X.; Xu, H.N. Preliminary study on chlorine fixation in combustion process of chemical pharmaceutical process residues. *Chem. Manag.* **2020**, *2020*, 175–224.
21. Luo, J.W.; Luo, X.L.; Zheng, X.S.; Chen, J.Y.; Liang, Y.Z.; Yang, Z.; Chen, Y. Simulation study on heat transfer equipment of organic Rankine cycle system. *J. Guangdong Univ. Technol.* **2022**, *39*, 128–134.
22. Lin, D.D. The Comprehensive Performance Evaluation and Working Fluid Selection of the Organic Rankine Cycle. Master's Thesis, Tianjin University, Tianjin, China, 2016.
23. Peng, B.; Liu, S.; Liu, H.X.; Zhou, T.H. Study on the influence of different working fluids on the performance of organic Rankine cycle low temperature thermal power generation system. *Therm. Power Gener.* **2021**, *51*, 43–48.
24. Xie, Z.Y.; Huang, G.D.; Jin, Q.; Ge, Z.; Yuan, Z.P. Effect of different working fluids on thermal performance of organic Rankine cycle system with built-in heat exchanger. *Renew. Energy* **2022**, *40*, 166–171.
25. Zhou, T.; Huang, Z.H.; Ding, X.L. The research and engineering application of organic Rankine cycle power generation system with high pressure temperature regulating water. *Therm. Power Gener.* **2022**, *51*, 27–34.
26. Li, J.; Yang, Z.; Duan, Y.Y. Organic Rankine cycle of non-azeotropic working fluid driven by medium-low temperature heat energy. *J. Tsinghua Univ. Nat. Sci. Ed.* **2022**, *62*, 693–703.
27. Liu, Z.; Liu, X.; Zhang, W.; Yang, S.; Li, H.; Yang, X. Thermodynamic analysis on the feasibility of a liquid energy storage system using CO₂-based mixture as the working fluid. *Energy* **2022**, *238*, 121759. [[CrossRef](#)]
28. Liang, J.W.; Luo, X.L.; Yang, Z.; Liang, Y.Z.; Chen, J.Y.; Chen, Y. Screening of mixed working fluids and optimization of organic Rankine cycle system based on PC-SAFT. *J. Guangdong Univ. Technol.* **2022**, *39*, 91–98.
29. Zhou, Y.; Zhang, R.; Wang, D.S. The improvement of performance comprehensive evaluation model based on analytic hierarchy process. *J. Anhui Open Univ.* **2022**, *2022*, 36–41.
30. Liu, D. Research on subjective evaluation index weight of vehicle ride comfort based on entropy method. *Traffic Energy Sav. Environ. Prot.* **2020**, *16*, 11–13.